QUANTIFICATION OF RESTING-STATE FMRI NETWORKS DRIVEN BY HEMODYNAMICALLY INFORMED SPATIOTEMPORAL REGULARIZATION

F. Işık Karahanoğlu[1,2]*, Camille Piguet* [3]*, Younes Farouj*[4,5]*, Patrik Vuilleumier*[3,6]*, Dimitri Van De Ville*[4,5]

[1] MGH/HST Athinoula A. Martinos Center for Biomedical Imaging, Massachusetts General Hospital, USA
[2] Department of Radiology, Harvard Medical School, MA, USA
[3] Department of Neuroscience, Faculty of Medicine, University of Geneva, Switzerland
[4] Department of Radiology and Medical Informatics, Faculty of Medicine, University of Geneva, Switzerland
[5] Medical Image Processing Laboratory, Ecole Polytechnique Fdrale de Lausanne (EPFL), Lausanne, Switzerland
[6] Swiss Center for Affective Sciences, Campus Biotech, Geneva, Switzerland

ABSTRACT

The brain's spontaneous fluctuations measured by functional magnetic resonance imaging during rest cluster into recurrent activity patterns known as resting-state networks (RSNs). The spatial organization of RSNs in health and disease has been immensely investigated by conventional correlational analyses of fMRI time series. Recent findings of time-resolved analyses have provided evidence of reoccurring activation patterns that are accessible at instantaneous time points enabling the dynamic characterization of RSNs. We have proposed a method to recover spatially and temporally overlapping RSNs, which we named innovation-driven co-activation patterns (iCAPs), to study the dynamic engagement of RSNs unconstrained by the slow hemodynamic response. The iCAPs are extracted by temporal clustering of sparse innovation signals recovered from Total Activation (TA) framework, which is cast as a variational problem with sparsity-promoting spatial and temporal priors for fMRI data deconvolution. The temporal prior uses the inverse of the hemodynamic response function as a general differential operator and exploits sparsity of the innovation signals. In this work, we perform a quantitative analysis to assess the stability of iCAPs recovered from a group of patients with mood disorders and healthy volunteers.

Index Terms— resting-state fMRI, deconvolution, mood disorders, total activation, innovation-driven co-activation patterns

1. INTRODUCTION

The blood-oxygen-level-dependent (BOLD) functional magnetic resonance imaging (fMRI) enables to measure the brain activity non-invasively by using the (de)oxygen concentration in the brain as an endogenous contrast agent [1]. As a result of neurovascular coupling, which accounts for the changes in blood volume, blood flow, and oxygen consumption in the vessels, the BOLD signal can be used to infer neuronal activity. A temporal model for neurovascular coupling, which relates neuronal activity to measured BOLD signal, was proposed by Buxton et al. through a non-linear differential system [2], whose simplified form, hemodynamic response function (HRF), allows for linear, time-invariant analysis [3–5].

During task fMRI, the conventional analyses rely on the timing information of the experimental paradigm, which is known a priori to the experiment. However, during resting-state fMRI, building a temporal fMRI model is challenging since there is no explicit task. Several static and dynamic methods have been proposed to extract information from the rs-fMRI data [6, 7]. The recent findings of dynamic fMRI analyses suggested recurring activation patterns; i.e., resting-state networks (RSNs), could be accessible at instantaneous time points in fMRI [8, 9]. We have proposed Total Activation (TA) framework based on a generative temporal fMRI model that represents activity-related signals as convolution of block-like activity-inducing signals and hemodynamic response function. TA is cast as an optimization problem with fMRI-tailored temporal and spatial regularization terms to denoise the fMRI signal and recover the underlying activity-inducing signals even in the absence of a task [10]. The deconvolved signal; i.e., block-like activity-inducing signals whose derivatives are sparse innovation signals, mimic neuronal activity. Furthermore, temporal clustering of the sparse innovation signals led to spatially and temporally overlapping resting-state networks, innovation-driven co-activation patterns (iCAPs) [11]. These activation patterns constitute the building blocks of rs-fMRI, where the activation of pattern at each time instance is represented as specific combination of iCAPs.

In this work, we evaluate the stability and inter-subject

This work was supported in part by the Swiss National Science Foundation (grant #205321_163376) to D.V.D.V. and F.I.K; CP was supported by a clinician-scientist grant from the Swiss National Center of Competence in Research, 'Synapsy: the Synaptic Basis of Mental Diseases' (grant #51NF40-158776)

spatial variability of iCAPs in a group of participants with mood disorders and healthy individuals.

2. METHODS

2.1. fMRI signal model

The forward model for the measured BOLD signal, $x(i,t)$, of i^{th} voxel can be expressed as convolution of system response; i.e., hemodynamic response function (HRF), and a block-like signal representing the neuronal activity

$$y(i,t) = x(i,t) + \epsilon(i,t) = u(i,t) * h(t) + \epsilon(i,t), \quad (1)$$

where $h(t)$ is the HRF, $\epsilon \sim \mathcal{N}(0, \sigma_i^2)$ is Gaussian noise, $u(i,t) = \sum_k c_k(i) b(t/a_k - t_k)$, is the block-like activity-inducing signal with weights c and step function $b(t)$.

2.2. Total activation

Total activation (TA) is cast as a spatiotemporal regularization problem to recover the underlying block-like activity-inducing signals by promoting the sparsity of their temporal derivatives; i.e, innovation signals, while ensuring spatially coherent activation. The general form of TA can be formulated with temporal and spatial regularization terms specifically tailored for fMRI signal model as

$$\tilde{\mathbf{x}} = \arg\min_{\mathbf{x}} \frac{1}{2}\|\mathbf{y} - \mathbf{x}\|_F^2 + \mathcal{R}_T(\mathbf{x}) + \mathcal{R}_S(\mathbf{x}). \quad (2)$$

The temporal regularization term, $\mathcal{R}_T$, uses a generalized total variation framework [12] and can be expressed as

$$\mathcal{R}_T(\mathbf{x}) = \sum_{i=1}^{V} \lambda_1(i) \left|\left|\Delta_L \{\mathbf{x}(i,\cdot)\}\right|\right|_1, \quad (3)$$

where $\Delta_L = \Delta\Delta_{HRF}$ is the generalized derivative operator representing the inverse of HRF obtained through Balloon model, Δ_{HRF}, combined with a first-order derivative operator Δ, and V is the number of voxels.

A possible spatial regularization term exploits a predefined brain parcellation with $\ell_{(2,1)}$-norm

$$\mathcal{R}_S(\mathbf{x}) = \sum_{t=1}^{N} \lambda_2(t) \left|\left|\Delta_{\text{Lap}} \{\mathbf{x}(\cdot,t)\}\right|\right|_{(2,1)}. \quad (4)$$

where Δ_{Lap} is the Laplacian operator, N is the number of time points [10, 13].

The regularization formulation in equation (2) induces sparsity of the innovation signals; i.e., derivative of activtiy-inducing signals $\Delta\{\mathbf{u}\}$ in the temporal domain, and promotes coherent activation within the regions of a predefined structural atlas through $\ell_{(2,1)}$-norm. Generalized forward-backward splitting algorithm can be used to solve the regularization problem in temporal and space domains [14].

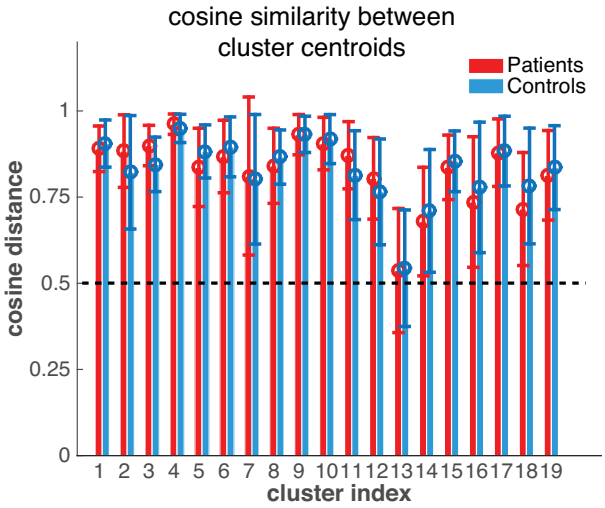

Fig. 1: The spatial stability of iCAPs. We performed 10 folds k-means clustering and computed the average similarity using cosine distance metric and standard deviation between each matching pair of cluster centroids; i.e., there are in total 45 pairs for 10 folds.

2.3. Innovation-driven co-activation patterns

The innovations represent brief moments of transient activations and carries the same information as the block-like activity-inducing signals. In order to recover coherent activation patterns that share the same innovation signals across subjects, the innovation signals were temporally concatenated and fed into temporal k-means clustering [11].

2.4. Spatial variability of iCAPs

First, we ran the k-means algorithm (k=20) using cosine distance as the similarity measure for 10 folds. We used 50 random k-means initializations where the minimum cost solution was picked as the most stable solution. We matched the group centroids between 10 solutions using Hungarian algorithm, and evaluated the similarity across folds. Then, instead of using cluster centroids, we evaluated the inter-subject similarity of iCAPs. We picked the best k-means solution and computed the subject-specific iCAPs, and measured the cosine similarity between each subject iCAP and group iCAP. Further, we drove a summary score per iCAP. We thresholded and created a binary mask for each subject-specific iCAP (z-score$\geq$1), and calculated the average percent overlap within the group iCAP divided by the average percent overlap outside of the group iCAP. This measure is expected to be higher ($>> 1$) when inter-subject spatial variability of that iCAP is low.

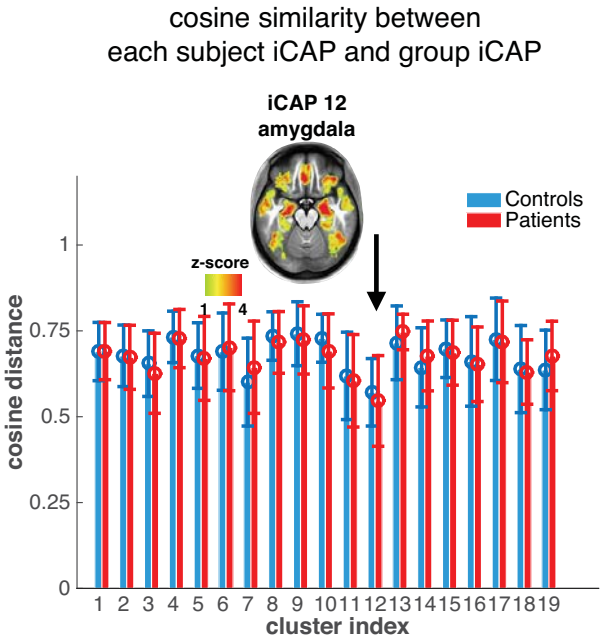

Fig. 2: The inter-subject variability. Using the best k-means solution performed on the whole dataset, we computed the cosine distance between subject-specific iCAPs and group iCAP. A subcortical network (iCAP 12, amygdala network) provided lowest score, however, there were no significant differences between the groups.

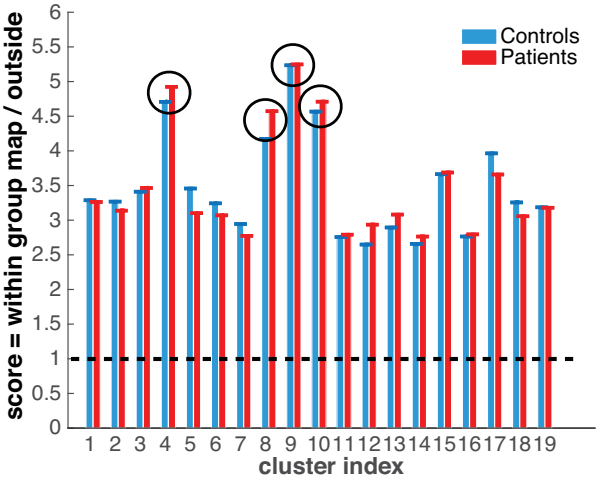

Fig. 3: Percent spatial overlap of iCAPs. Each subject-specific iCAP was binarized (z-score$\geq$1), and percent spatial overlap within and outside of the group iCAP was computed. All iCAPs provided high overlap (scores $>>$1), and there were no differences across the groups.

3. RESULTS

3.1. Data Acquisition and Preprocessing

The study was conducted at the Geneva University Hospital. All participants gave informed written consent in accordance with procedures approved by the Ethics Committee of the Geneva University Hospital. The MRI data was acquired with Siemens 3T Trio scanner using 32 channel head coil. The resting-state fMRI data were collected using 2D gradient-echo echo-planar (EPI) sequence with the following protocol parameters: 36 transverse slices covering the whole brain, voxel size = $3.2\times3.2\times3.2$ mm^3, acquisition matrix = 64×64, FOV = 205 mm, TR/TE/FA = 2100 ms/30 ms/90^o, 250 volumes). The total acquisition took around 8.5 mins. The MRI data were acquired from 31 mood disorder patients (depression score [0-33]: 13.7 ± 9.5) and 32 healthy volunteers (depression score [0-33]: 1.9 ± 1.8) matched for age, gender, laterality, and level of education.

The fMRI data were preprocessed using custom MATLAB code combined with SPM8 (FIL, UCL, UK) and IBASPM toolboxes [15]. The first 10 volumes were discarded for magnetization stability, and time series were detrended for baseline, first order and low frequency drifts (cut-off: 0.008Hz). The fMRI volumes were realigned to the mean volume and spatially smoothed with Gaussian filter (full width half maximum=3mm). We used motion estimation to mark the time points with excessive amount of motion (max motion $\geq$ 3 mm or frame-wise displacement $\geq$ 0.5 mm) [16]. Marked frames were not removed as TA requires uniform temporal sampling, therefore, we performed cubic-spline interpolation to high motion frames and their one neighborhood frames. Five healthy subjects and four patients were excluded from further analysis, therefore, our analysis consisted twenty seven individuals in both groups.

The structural images were coregistered to the mean functional volume and segmented (NewSegment, SPM8) for the six different MNI templates. The anatomical automatic labelling atlas, composed of 90 regions without the cerebellum, was mapped onto each subject's coregistered anatomical image and further downsampled to match the functional images. The TA analysis was run on each subject's functional space, and the atlas was used to guide TA's spatial regularization. The resulting activity-inducing and innovation signals were normalized to MNI space using the deformation matrix in the segmentation step.

3.2. Stability of group-level iCAPs

We have opted for 20 clusters, however, one cluster were represented only in one subject, so left out from the analysis.

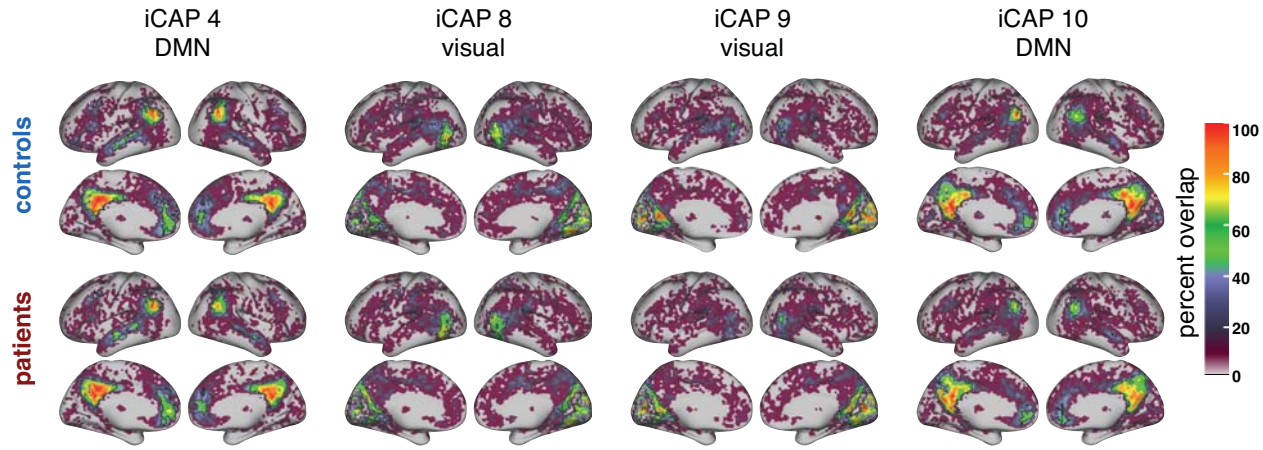

Fig. 4: The spatial localization of the dominant iCAPs. DMN and visual networks were the most dominant iCAPs with maximum overlap across subjects within group the iCAP mask. The black circles show the outline of group iCAPs.

Fig. 1 depicts the stability of the clusters across 10 k-means (for 10 folds we have $\binom{10}{2} = 45$ metrics for each cluster). The cluster similarity measurements provide an insight on the spatial reproducibility. Although one cluster (iCAP 13, visual network) showed relatively low scores compared to others, both patients and controls showed similar stability measurements.

3.3. Inter-subject variability

Fig. 2 shows the average similarity between each subject's iCAP and the group iCAP. Again, there were no group differences in the inter-subject variability. One subcortical network (iCAP12, amygdala network) showed lowest score compared to others perhaps due to small amount of voxels spanned in those networks or higher spatial variability in subcortical regions.

We have further assessed the inter subject variability in Fig. 4 using a summary score reflecting the average percent overlap of voxels within the group iCAP and voxels outside of the group iCAP. We have specifically found four dominant networks of which almost all subjects contribute to the group maps (Fig. 3, iCAPs 4–10, default-mode network (DMN), and iCAPs 8–9, visual networks).

4. DISCUSSION

In this work, we have conducted a quantitative analysis of the subject-specific spatial variability of iCAPs in mood disorder patients healthy controls. We have found reproducible patterns in all iCAPs, of which subcortical networks showed higher inter-subject variability. The visual networks and two DMN showed very high spatial localization. We have not found any differences between the groups in terms of spatial consistency.

5. REFERENCES

[1] S Ogawa, R S Menon, D W Tank, S G Kim, H Merkle, J M Ellermann, and K Ugurbil, "Functional brain mapping by blood oxygenation level-dependent contrast magnetic resonance imaging. a comparison of signal characteristics with a biophysical model," *Journal of Biophysics*, vol. 64, no. 3, pp. 803–12, Mar 1993.

[2] R. B. Buxton, E. C. Wong, and L. R. Frank, "Dynamics of blood flow and oxygenation changes during brain activation: The Balloon model.," *Magnetic Resonance in Medicine*, vol. 39, no. 6, pp. 855–864, Jun 1998.

[3] K. J. Friston, P. Fletchera, O. Josephs, A. Holmes, M. D. Rugg, and R. Turner, "Event-Related fMRI: Characterizing Differential Responses," *NeuroImage*, vol. 7, no. 1, pp. 30–40, Jan. 1998.

[4] K. J. Friston, A. Mechelli, R. Turner, and C. J. Price, "Nonlinear responses in fMRI: The balloon model, Volterra kernels, and other hemodynamics," *NeuroImage*, vol. 12, no. 4, pp. 466 – 477, 2000.

[5] I. Khalidov, D. Van De Ville, J. Fadili, and M. Unser, "Activelets and sparsity: A new way to detect brain activation from fMRI data," in *Proceedings of the SPIE Conference on Mathematical Imaging: Wavelet XII*, San Diego CA, USA, August 26-29, 2007, vol. 6701, pp. 1–8.

[6] R. M. Hutchison, T. Womelsdorf, E. A. Allen, P. A. Bandettini, V. D. Calhoun, M. Corbetta, S. Della Penna, J. H. Duyn, G. H. Glover, J. Gonzalez-Castillo, D. A.

Handwerker, S. Keilholz, V. Kiviniemi, D. A. Leopold, F. de Pasquale, O. Sporns, M. Walter, and C. Chang, "Dynamic functional connectivity: Promise, issues, and interpretations," *NeuroImage*, vol. 80, no. 0, pp. 360 – 378, 2013.

[7] Shella Keilholz, Cesar Caballero-Gaudes, Peter Bandettini, Gustavo Deco, and Vince Calhoun, "Time-resolved resting-state functional magnetic resonance imaging analysis: Current status, challenges, and new directions," *Brain Connectivity*, vol. 7, no. 8, pp. 465–481, 2017, PMID: 28874061.

[8] Maria Giulia Preti, Thomas Bolton, and Dimitri Van De Ville, "The dynamic functional connectome: State-of-the-art and perspectives," *NeuroImage*, in press.

[9] Fikret Isik Karahanoglu and Dimitri Van De Ville, "Dynamics of large-scale fmri networks: Deconstruct brain activity to build better models of brain function," *Current Opinion in Biomedical Engineering*, vol. 3, pp. 28 – 36, 2017, New Developments in Biomedical Imaging.

[10] F. I. Karahanoglu, C. Caballero-Gaudes, F. Lazeyras, and D. Van De Ville, "Total activation: fMRI deconvolution through spatio-temporal regularization," *NeuroImage*, vol. 73, pp. 121 – 134, 2013.

[11] F. I. Karahanoğlu and D. Van De Ville, "Transient brain activity disentangles fMRI resting-state dynamics in terms of spatially and temporally overlapping networks.," *Nature Communications*, vol. 6, pp. 7751, 2015.

[12] F. I. Karahanoglu, I. Bayram, and D. Van De Ville, "A signal processing approach to generalized 1-D total variation," *IEEE Transactions on Signal Processing*, vol. 59, no. 11, pp. 5265 –5274, November 2011.

[13] Younes Farouj, Fikret Isik Karahanoglu, and Dimitri Van De Ville, "Regularized spatiotemporal deconvolution of fmri data using gray-matter constrained total variation," in *14th IEEE International Symposium on Biomedical Imaging, ISBI 2017, Melbourne, Australia, April 18-21, 2017*. 2017, pp. 472–475, IEEE.

[14] H. Raguet, J. Fadili, and G. Peyre, "A generalized forward-backward splitting," *SIAM Journal on Imaging Sciences*, vol. 6, no. 3, pp. 1199–1226, 2013.

[15] Y. Alemán-Gómez, L. Melie-Garćia, and P. Valdés-Hernandez, "IBASPM: Toolbox for automatic parcellation of brain structures," *12th Annual Meeting of the Organization for Human Brain Mapping*, vol. 27, 2006.

[16] J.D. Power, A.B. Kelly, Z.S. Abraham, L.S. Bradley, and E.P. Steven, "Spurious but systematic correlations in functional connectivity mri networks arise from subject motion," *NeuroImage*, vol. 59, no. 3, pp. 2142–2154, 2012.